

Tolperisone – a Novel Modulator of Ionic Currents in Myelinated Axons

D HINCK AND E KOPPENHOFER

*Institute of Physiology University of Kiel,
Kiel, Germany*

Abstract. The actions of tolperisone on single intact Ranvier nodes of the toad *Xenopus* were investigated by means of the Hodgkin-Huxley formalism. Adding tolperisone to the bathing medium (100 $\mu\text{mol/l}$) caused the following fully reversible effects:

- 1 The sodium permeability P'_{Na} was decreased by about 50% in a nearly potential-independent manner while the so-called sodium inactivation curve was shifted in the negative direction by about 3 mV.
- 2 The remaining parameters of the sodium system, i.e. m , τ_m and τ_h , did not change.
- 3 The potassium permeability P'_K decreased at strong depolarizing potentials ($V > 60$ mV), hence the permeability constant \bar{P}_K decreased by about 8%. However, weak depolarizations ($V < 60$ mV) caused P'_K to increase by about 7%.
- 4 The potassium activation curve was shifted in the positive direction by about 9 mV and the exponent of n , b , was reduced from about 3.5 to about 1.5.

Concentration-response relations for reduction of the sodium permeability constant \bar{P}_{Na} and of the potassium permeability constant \bar{P}_K yielded apparent dissociation constants of about 0.06 mmol/l and 0.32 mmol/l, respectively. The increase of P'_K at $V = 40$ mV, however, was largely concentration-independent.

Our findings show that, in contrast to the prevailing view, tolperisone cannot be said to have a so-called lidocaine-like activity, because its effect on potassium permeability in the threshold region is fundamentally different from that of other known local anaesthetics. We infer that this effect, in combination with the decrease in sodium permeability, is responsible for the tendency of tolperisone to reduce excitability and hence for the antispastic action of tolperisone documented by clinical observations.

Key words: Tolperisone — K⁺-channel modulator — Node of Ranvier — Anti spastic drug

Introduction

Spasticity, in the sense of a prolonged pathologically elevated tone of skeletal muscles, frequently causes severe pain to those affected, particularly in cases of multiple sclerosis (MS) (Jellinger 1984). It is often possible to alleviate their suffering rapidly by administering suitable potassium-channel blockers, which as a specific symptomatic therapy for demyelinating diseases can compensate for the deterioration of impulse conduction in demyelinated axons. A particularly suitable agent for this purpose is 5-methoxypsoralen (5-MOP), because it presents a low risk of undesirable side effects. The efficacy of 5-MOP in MS, as well as in myelin-sheath defects of quite different origins, has been examined in several previous single-case studies (Bohuslavizki et al 1993b, 1995, Bautz'as et al 1995, Ditzel et al 1995, Koppenhofer et al 1995, Bautz et al 1996, Hansel et al 1998), which in turn provided an incentive for extensive *in vitro* investigations (Bohuslavizki et al 1993a, 1994b, During et al 1997, Mix et al 1998, Wissel et al 1998, Wulff et al 1998 a,b).

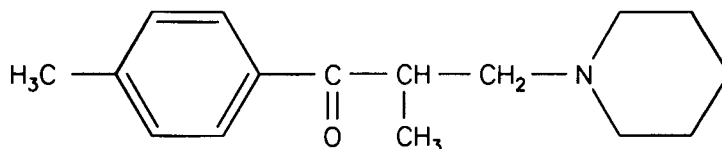


Figure 1. Molecular structure of tolperisone

Another drug, tolperisone (see Fig 1), has also been thought to have an anti-spastic action, in particular for MS patients (Lehoczy 1961, Hift and Sluga-Gasser 1962, Szobor 1993). Because its structure resembles that of the local anaesthetic lidocaine (Fels 1996), tolperisone has been said to have "lidocaine-like activity", implying that tolperisone acts like a typical local anaesthetic in blocking primarily the sodium channels of axonal membranes, it has been proposed that this so-called membrane stabilizing action may participate in spinal reflex inhibition produced by tolperisone (Ono et al 1984, Morikawa et al 1987).

The objective of the present study was to test this hypothesis about the action of tolperisone in *in vitro* experiments on intact myelinated axons. In particular, we wanted to clarify whether the antispastic action of tolperisone, as exhibited e.g., in MS, is likely to reside in an ability to block potassium channels, perhaps resembling that of 5-MOP. Some of the results of this study have been reported previously (Hinck and Koppenhofer 1997).

Materials and Methods

Preparation and experimental setup The experiments were done on isolated myelinated nerve fibres (median diameter $24.3 \mu\text{m}$, range 20.3 to $28.4 \mu\text{m}$, $N = 10$) from the sciatic nerve of the toad *Xenopus laevis*. Membrane currents were measured by a state-of-the-art potential clamp system (Bethge et al 1991, Bohuslavizki et al 1994a, Zaciú et al 1996). Nevertheless, some spontaneous changes were still inevitable. Therefore before control data were obtained in the normal bathing medium, i.e. before and after application of a test solution, all the technologically accessible parameters that could influence the scatter of data were checked and, where necessary, readjusted (for details, see Düring et al 2000). This allowed experiments to be continued for several hours with no rundown that measurably affected the results. This in turn brought considerable savings in the number of experiments and thus also in time and funds (Bethge et al 1991, Hinck et al 2001).

Measurement conditions and calibrations For current-voltage relations various positive test pulses V at a repetition rate of 1 Hz were preceded by appropriate negative prepulses, so that at the beginning of each test pulse the sodium inactivation variable h was unity. For sodium inactivation curves the steady-state value of h was measured by the well-known two-pulse protocol (Frankenhaeuser 1959). Specific currents were calculated from membrane current records and from fibre dimensions (Stampfli and Hille 1976). In order to record action potentials, the measurement system was switched to the current-clamp configuration so that suitable stimulus pulses could be administered.

Data processing Membrane current recordings were corrected automatically for leakage currents, filtered by a low-pass fourth-order Bessel filter (corner frequency 40 kHz) and digitized by a 12 bit A/D converter at 250 kHz (Bethge et al 1991). To obtain adequate signal/noise ratios even at weak depolarisations ($V \leq 40$ mV) the technique of signal averaging was employed. 16 current recordings elicited by identical test pulses V at a repetition rate of 1 Hz (jitter < 100 ns) were averaged together to form a single mean time course, the ensemble average (Albers et al 1989). In addition, for further noise reduction where necessary, the signal was digitally filtered in such a way as to obtain a linear average over 5 to maximally 17 data points at a constant converting rate. The transmission characteristics thus obtained are shown in Fig. 2. In particular for broad data windows (∇), the filter curve is clearly non-monotonic, this results from the uniform weighting of the data points and caused us to use digital filtering only very sparingly.

To calculate the membrane permeabilities P_{Na} and P_{K} from the underlying ionic currents the constant-field concept was applied (Bohuslavizki et al 1994b). The permeability constants \bar{P}_{Na} and \bar{P}_{K} were found by calculation of P'_{Na} and P'_{K} , respectively, by means of least square fitting from the time course of the current recordings.

In determining P'_{Na} the disturbing influence of the superimposed potassium currents was reduced by neglecting the 25–30% close to zero of the peak sodium

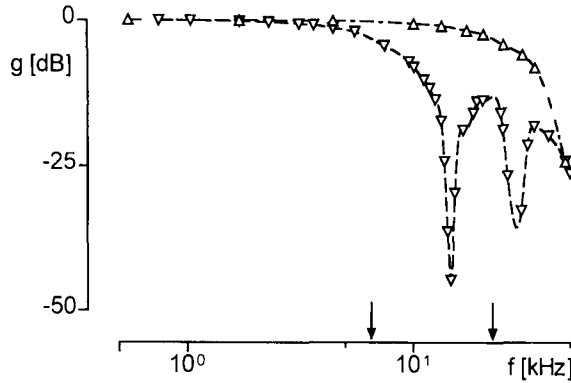


Figure 2 Transmission characteristics of the digital filter employed. Ordinate: attenuation of sine wave amplitudes g , in dB. Abscissa: test frequencies f in kHz with A/D conversion at 250 kHz. Window widths: 5 data points (Δ), 17 data points (∇). The arrows denote the apparent corner frequencies (-3 dB) of the respective filter settings. Linear interpolation.

current in each case (Bohuslavizki et al. 1994b). We applied the simplified equation (Bohuslavizki et al. 1994a)

$$P'_{Na} = P'_{Na} [1 - \exp(-t - \delta t)/\tau_m] \exp(-t - \delta t)/\tau_h \quad (1)$$

with

$$P'_{Na} = \bar{P}_{Na} m_{\infty} \quad (2)$$

here the parameters have their usual meaning (Frankenhaeuser 1960; During et al. 2000; Hinck et al. 2001). For sodium permeability curves the P'_{Na} values were plotted *versus* test pulse amplitude V and fitted by the equation

$$P'_{Na} = \bar{P}_{Na} \frac{1}{1 + \exp[(V_{PNa} - V)/k_{PNa}]} \quad (3)$$

(Bohuslavizki et al. 1994a; During et al. 2000; Hinck et al. 2001) here V_{PNa} represents the position of the inflection point of the curve on the potential axis, k_{PNa} is the maximal slope and \bar{P}_{Na} is the extrapolated maximum of the calculated curve. Note that after setting $\bar{P}_{Na} = 1$, Eq. (3) is numerically identical to the corresponding sodium activation curve, m_{∞} *versus* V (Frankenhaeuser 1960; Albers et al. 1989).

The simple procedure for separating sodium from potassium currents described above, by delimiting the evaluated potential and time ranges in the current recordings, does not provide any useful data on potassium activation. For this reason the subtraction method proposed by Hinck and coworkers (Hinck et al. 2001) was

employed for this purpose. In this method all current recordings made in ordinary Ringer solution, as well as those under tolperisone, were replicated: once with gallamine triethiodide added to the bathing solution and once without. In the potential range of interest here, gallamine at 1 mmol/l is an almost perfect selective potassium blocker, eliminating more than 90% of the potassium currents at the membrane of the Ranvier node (Hinck et al. 2001). Hence subtraction of these sodium-only recordings from the corresponding non-gallamine recordings, in Ringer solution or under tolperisone, reveals the shape of the potassium currents after the sodium currents have been eliminated. For curve fitting we used the simplified equation

$$P_K = P'_K \cdot [1 - \exp(-t - \delta t)/\tau_n]^b \quad (4)$$

with

$$P'_K = \bar{P}_K \cdot n_\infty^b \quad (5)$$

(Frankenhaeuser 1963). Note that for δt in this case the numerical values found previously from the curve fittings with Equation (1) were used.

It is known that the potential dependence of P'_K does not conform to a sigmoid curve (Frankenhaeuser 1962; Bohuslavizki et al. 1994b; Düring et al. 2000; Hinck et al. 2001). Therefore for potassium permeability curves the data that describe the decay of P'_K at strong depolarizations ($V \geq 100$ mV) were discarded and the remaining data were fitted by an equation corresponding to Equation (3), namely

$$P'_K = \bar{P}_K \frac{1}{1 + \exp[(V_{PK} - V)/k_{PK}]} \quad (6)$$

so that the value extrapolated from the calculated curve gave the permeability constant \bar{P}_K . Repetition of this procedure with $\bar{P}_K = 1$, taking into account that $b \neq 1$, finally gives the potassium activation curve, n_∞ versus V .

In order to quantify the blocking properties of tolperisone, blockages of \bar{P}_{Na} and \bar{P}_K were defined as

$$B_{Na} = \frac{\Delta \bar{P}_{Na}}{\bar{P}_{Na \text{ control}}} \quad (7)$$

with

$$\Delta \bar{P}_{Na} = \bar{P}_{Na \text{ control}} - \bar{P}_{Na \text{ test}}$$

and

$$B_K = \frac{\Delta \bar{P}_K}{\bar{P}_{K \text{ control}}} \quad (8)$$

with

$$\Delta \bar{P}_K = \bar{P}_{K \text{ control}} - \bar{P}_{K \text{ test}}$$

respectively and plotted semilogarithmically against the test concentration c . The data were fitted with the equations

$$B_{Na} = \frac{B_{Na \text{ max}} \cdot c^x}{c^x + B_{Na \text{ C50}}} \quad (9)$$

and

$$B_K = \frac{B_{K \max} \cdot c^y}{c^y + B_{K C50}} \quad (10)$$

(Hinck et al 2001). The fits yielded values for the apparent dissociation constants of blockage, $B_{Na C50}$ and $B_{K C50}$, and for the respective steepness parameters x and y .

As a measure of quality of the curve fitting we used the nonlinear regression coefficient r_{nl} (Sachs 1984). It was at least 0.9805.

Chemicals and solutions. The normal bathing medium was Ringer solution (in mmol/l): NaCl 107.0; KCl 2.5; CaCl₂ 2.0; N,N bis (hydroxyethyl)-2-aminomethanesulfonic acid/Na OH buffer (BES) 5.0. Test solutions were produced by adding tolperisone (2,4'-dimethyl-3-piperidinopropiophenone) as the hydrochloride (kindly supplied by Strathman AG, Hamburg, Germany) to the Ringer solution in an amount such that the test concentration was 100 μ mol/l if not stated otherwise. In some experiments, to both Ringer solution and test solution the potassium channel blocker gallamine triethiodide (2,2',2''-[1,2,3-benzenetriyltris (oxy)] tris [N,N,N-triethylethanaminium] triiodide) (Sigma-Aldrich Chemie, Steinheim, Germany) was added in an amount such that in both solutions the gallamine concentration was 1 mmol/l (see page 417). The pH of all solutions was 7.2; the temperature was 10°C.

Results

Current-voltage relations. The membrane currents elicited by positive test pulses conformed to the known time course (Dodge and Frankenhaeuser 1958) and were unchanged by tolperisone (not shown). The potential dependence of the peak

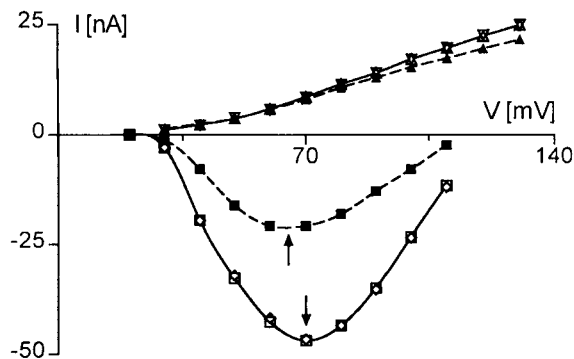


Figure 3. Current voltage relations of peak sodium currents (squares and diamonds) and of steady-state potassium currents (triangles) before and after application of test solution (open symbols) and under tolperisone (filled symbols) Test concentration 100 μ mol/l The curves were obtained by spline interpolation The arrows denote the maximum of the respective curves on the potential axis All data from one individual experiment

sodium currents and the steady-state potassium currents is shown in Fig. 3. Under tolperisone (filled symbols) there is a completely reversible, marked decrease in the peak sodium currents (median: by 48%; range: 37.9–63%; $N = 16$) and a less pronounced decrease in the steady state potassium currents (at $V = 130$ mV; median: by 18%; range 6–21%; $N = 16$). Furthermore, the maximum of the peak sodium current-voltage relation (dashed line) is shifted in the negative direction (median: by 5 mV; range: 0.0–6.5 mV; $N = 16$).

Parameters of the sodium permeability. The curve fittings with Eq. (1) produced numerical values not only for the permeability P'_{Na} (Fig. 6A) but also for m_{∞} and the time constants τ_m and τ_h (Fig. 4) as well as the so-called delay time δt of the measuring system (Fig. 10). P'_{Na} was about halved by tolperisone in a potential-independent manner while the potential-dependence curves for τ_m , τ_h and m_{∞} have the well-known shape and were not clearly influenced; a striking feature of the τ_m and τ_h curves, however, is a remarkable increase in the scatter of the data during weak depolarizations. The inactivation curve, on the other hand, was clearly

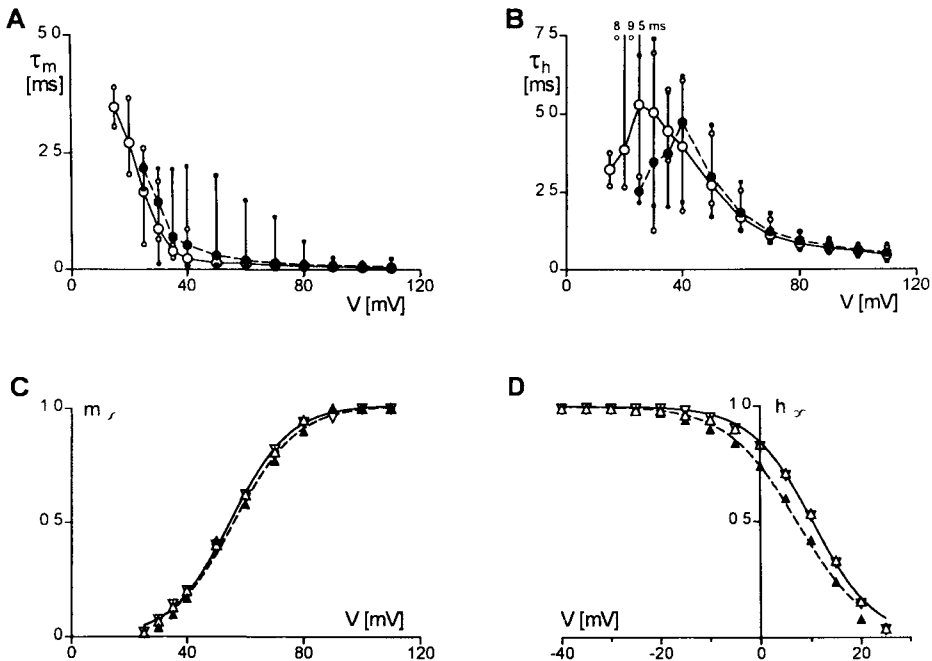


Figure 4. Potential dependence of parameters of the sodium permeability. Note that τ_m , τ_h and m_{∞} were found by curve fitting while h_{∞} was measured conventionally (see page 415). Open symbols, normal Ringer solution, filled symbols, under tolperisone. **A.**, **B.** linear interpolation, medians and ranges, $N = 12$. **C.**, **D.** curves were calculated by Eq. (2) this paper and by Eq. (6) from Bohuslavizki and coworkers (1994b), respectively, two typical experiments.

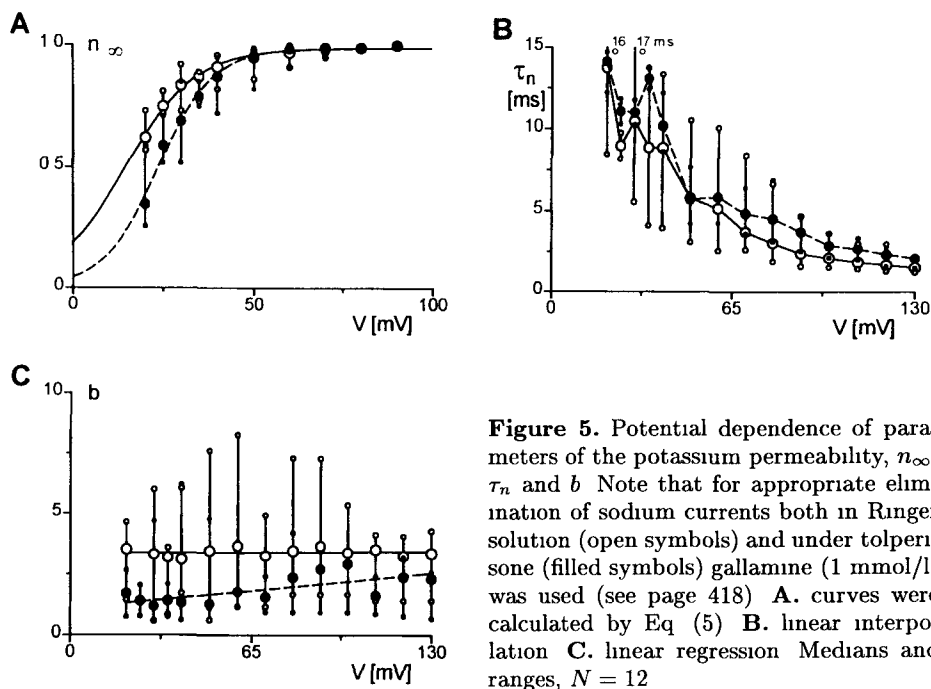


Figure 5. Potential dependence of parameters of the potassium permeability, n_{∞} , τ_n and b . Note that for appropriate elimination of sodium currents both in Ringer solution (open symbols) and under tolperisone (filled symbols) gallamine (1 mmol/l) was used (see page 418). **A.** curves were calculated by Eq (5) **B.** linear interpolation **C.** linear regression Medians and ranges, $N = 12$

shifted in the negative direction by tolperisone (median: by 4.1 mV; range: 4.5–3.0 mV; $N = 3$).

Parameters of the potassium permeability The curve fittings with Eq (4) produced numerical values not only for the permeability P'_K but also for n_{∞} , τ_n and the exponent of n , b . The potassium activation curves (Fig. 5A) were measurable only down to $V = 20$ mV even though all technically possible means of noise reduction (see page 415) were employed; hence the fitting of curves to the data by means of Eq (5) gave only approximate values for n_{∞} at the resting potential ($V = 0$). The potential dependence of the time constant τ_n had the known shape (B). As observed for the time constant of sodium permeability, however, the scatter of the data increased markedly and largely masked the slight increase in τ_n caused by tolperisone (filled symbols). The exponent b (C) was independent of potential under control conditions (open symbols), with a value of about 3.5 as previously published (Koppenhöfer 1967). Under tolperisone (filled symbols) it fell to about 1.5. Here again, as in B, the data are surprisingly widely scattered, especially under control conditions.

Permeability-voltage curves For sodium permeability curves (Fig. 6A) Eq. (3) was fitted to the P'_{Na} values measured in Ringer solution. The extrapolated maximum of the calculated curve gave the permeability constant \bar{P}_{Na} in Ringer solution, which was then used to normalize the values of P'_{Na} found for Ringer solution and

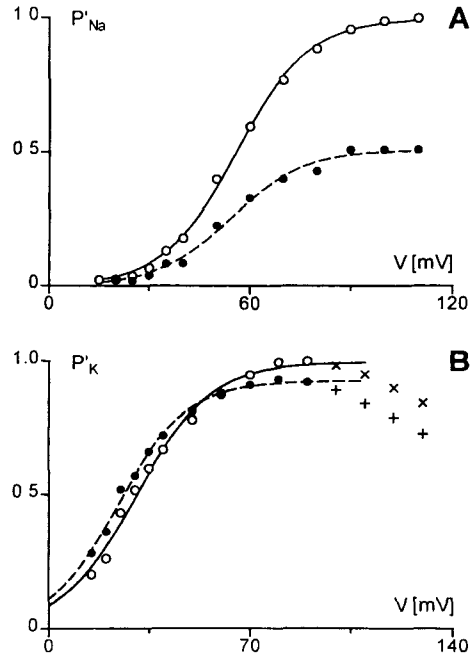


Figure 6. Potential dependence of membrane permeabilities in Ringer solution (open symbols) and under tolperisone (filled symbols). **A.** sodium permeability P'_{Na} ; ordinate: P'_{Na} as normalized to the maximum of the continuous curve, which was fitted to the data in Ringer solution; both curves were calculated by Eq. (3). **B.** potassium permeability P'_K ; ordinate: P'_K as normalized to the maximum of the continuous curve, which was fitted to the data in Ringer solution; both curves were calculated by Eq. (6). Note that the data denoting the decay of P'_K during strong depolarizations were neglected. Medians; $N = 7$ and 9 , respectively.

for the test solution as well. Then Eq. (3) was fitted to the latter values, which gave the permeability constant \bar{P}_{Na} under tolperisone. The reduction of P'_{Na} by tolperisone ($100 \mu\text{mol/l}$) was nearly potential-independent and amounted for \bar{P}_{Na} to 47% (median; range: 29–53%; $N = 7$).

The same procedure was used for potassium permeability curves (Fig. 6B), except that the values found for the decline of P'_K following strong depolarizations were not included in the fitting of Eq. (6) to the data. The extrapolated maximum of the calculated curve gave the permeability constant \bar{P}_K in Ringer solution, which was then used to normalize the values of P'_K found for both Ringer and test solution. Then Eq. (6) was fitted to the latter values, which gave the permeability constant \bar{P}_K under tolperisone. The reduction of \bar{P}_K by tolperisone ($100 \mu\text{mol/l}$) amounted to 8% (median; range: 2–15%; $N = 9$). Surprisingly, with weaker depolarizations the decrease in P'_K was converted to an increase, so that the two calculated curves intersected one another at about $V = 60$ mV. The increase in P'_K at $V = 40$ mV was 7% (median; range: 0–20%; $N = 9$).

Concentration-response relations. In order to obtain concentration-response relations the values of B_{Na} and B_K , obtained for blocking of \bar{P}_{Na} and \bar{P}_K , respectively, were examined at various test concentrations (Fig. 7). The same procedure was followed for the B_K values calculated from the P'_K values measured at $V = 40$ mV. Fitting of Eq. (9) to the B_{Na} values (A, ●) and of Eq. (10) to the B_K values cal-

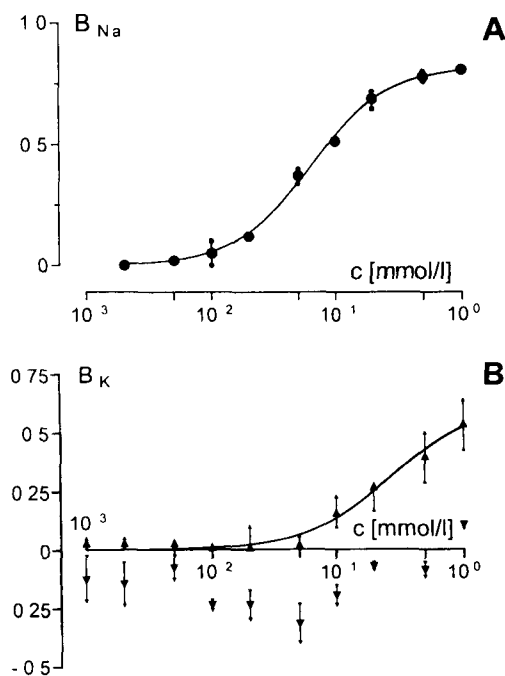


Figure 7. Concentration-response relations for the blocking of sodium permeability (A) and potassium permeability (B) by tolperisone. Ordinate **A** block of the sodium permeability constant \bar{P}_{Na} , B_{Na} , (●) according Eq (7) **B** block of the potassium permeability P_K , B_K , defined either as $P_K = \bar{P}_K$ (▲) or as $P_K = P'_K$ at $V = 40$ mV (▼). The curves were calculated by Eq (9) and (10), respectively, and fitted to the data. Medians and ranges, $N = 3$.

culated from P'_K (B, ▲) showed that in both cases high tolperisone concentrations make complete blocking impossible. The apparent dissociation constants amounted to $B_{Na C50} = 0.06$ mmol/l at $x = 1.4$ and $B_{K C50} = 0.32$ mmol/l at $y = 1.3$ (medians; $N = 3$). The increase in P'_K at $V = 40$ mV already visible in Fig. 6 exhibited a curious change within the concentration range tested here (Fig. 7B, ▼), whereas the above-mentioned slight increase in P'_K (= decrease in B_K) was confirmed, there was no discernible concentration-dependence of the effect that would have enabled curve fitting with Eq. (10).

Discussion

*Tolperisone – a typical local anaesthetic*² The action of tolperisone on the ion currents at the node of Ranvier of the toad consists in a marked, reversible blocking of the sodium currents and a reversible but considerably weaker blocking of the potassium currents. In this regard, and also with respect to the observed frequency dependence of the spike amplitude (see Fig. 8), the action of tolperisone corresponds closely to that of many local anaesthetics. Hence tolperisone can be said to resemble lidocaine not only in a structural (Fels 1996) but also in a functional sense, even though the apparent dissociation constants for sodium and potassium blocking by tolperisone are a good order of magnitude smaller than those by lidocaine (Århem and Frankenhaeuser 1974). Our assessment of the kinetics of the sodium

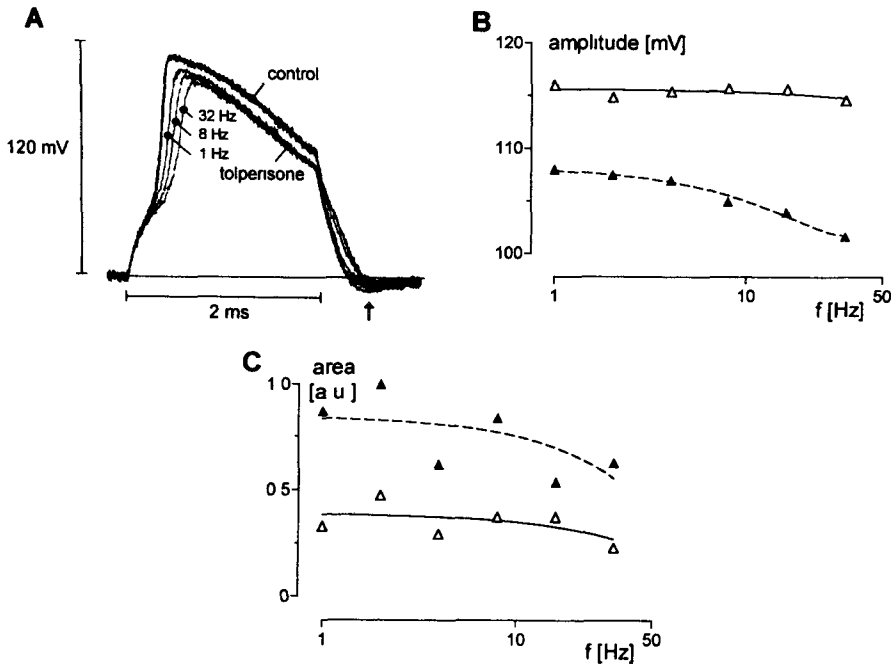


Figure 8. Frequency dependence of the effects of tolperisone (100 $\mu\text{mol/l}$) on action potentials **A.** time course of action potentials in Ringer solution (control) and under tolperisone (test) Constant stimulus strength 10 mV, 2 ms Repetition rate 1 to 32 Hz Note increase of negative afterpotentials under tolperisone (arrow) **B.** spike amplitudes in Ringer solution (open triangles) and under tolperisone (filled triangles) *versus* repetition rate **C.** surface area underneath negative afterpotentials in Ringer solution (open triangles) and under tolperisone (filled triangles) in arbitrary units *versus* repetition rate Data from one typical experiment

currents was hampered by an unusually broad scatter of the data (see Fig. 4). On the other hand, a marked blocking of sodium permeability by tolperisone was clearly evident, although the sodium activation curve was not affected. Both of these results also indicate a general functional similarity between tolperisone and typical local anaesthetics. However, the leftward shift of the sodium inactivation curve found here under tolperisone should not be interpreted in this sense, because although such a response is observed with practically every local anaesthetic, it is an unspecific characteristic of almost all neuropharmaceuticals that affect axonal sodium channels.

The main action of tolperisone on the parameters of potassium permeability, apart from a slight reduction of the exponent b , is to shift the potassium activation curve to the right and to produce a remarkable intersection of the potassium permeability curves, which to our knowledge has not yet been described in the literature: whereas during large depolarizations tolperisone seems to be a relatively

weak potassium-channel blocker, resembling typical local anaesthetics only in this regard (for references, see Strichartz 1987), slight depolarizations in the region of the threshold potential increase potassium permeability. Extrapolation of the P'_K curves (Fig 6B) and of the potassium activation curve (Fig 5A) to $V = 0$ indicates that in the presence of tolperisone the normalized potassium permeability $P'_K (V = 0)$ increases, whereas $n_\infty (V = 0)$ clearly decreases. None of this is typical of the action of known local anaesthetics.

Do our results match the properties of antispastic drugs? The pharmacological therapy of neurogenic spasticity consists in reducing the pathologically elevated activity in spinal reflex pathways (Young 1994). An action of this kind has been demonstrated for tolperisone in the rat (Ono et al 1984, Farkas et al 1989). It can be explained by the decreased sodium permeability of myelinated axons described here, that is, in the exemplary cases we tested ($N = 3$), the amplitude of the action potentials was decreased (see Fig 8A) so that there was a so-called tonic blocking of nerve conduction (Raymond 1992), the expected result of which would be an excitability-diminishing modulation of excitation patterns in reflex pathways, in the sense of a "temporal dispersion" (Waxman 1987). The observed frequency-dependent nature of action potentials under tolperisone (B) is typical of many substances and has long been known (Courtney 1975). This so-called phasic blocking of the action potentials would be expected to diminish excitability in general, especially in cases of pathologically increased reflex activity, and thus to have an antispastic action. Another consideration is that the inactivation of sodium permeability in sensory axons differs from that in motor axons (Bretag and Stampfli 1975), which might imply that tolperisone has a stronger excitability-reducing action in sensory axons. Although the sensitivity of motor and sensory axons to local anaesthetics is thought to be the same (Matthews and Rushworth 1957), it increases as the discharge rate rises (Sotgiu et al 1992), and sensory axons accommodate less than motor axons (Honerjager 1968), which allows pain stimuli to be encoded in the form of higher discharge rates. Therefore *in vivo* the sensory axons could indeed be more sensitive than motor axons to tolperisone, particularly in view of the special form of frequency dependence thus produced (see below).

To answer the question of the extent to which the altered parameters of potassium permeability demonstrated here also diminish the excitability of the axonal membrane, especially in the threshold region, it could be helpful to carry out computer simulations of the threshold conditions based on the data presented here. It should be taken into account, however, that the distribution of potassium channels in the axons of cold-blooded animals differs from that in humans (for references, see During et al 2000), and also that according to our observations tolperisone affects neither the leak conductance nor the resting potential at the node of Ranvier (not shown).

Regarding the only slight stimulus-frequency-dependent increase of the negative afterpotential at the end of the action potential (see Fig 8C), we ascribe this to the greater potential-dependent potassium permeability in the region of the

resting potential. The result expected *in vivo* would be a prolonged refractory period, which in turn would decrease excitability especially in cases of pathologically elevated spike frequencies – that is, in the sense of the above-mentioned “temporal dispersion”. Remarkably, however, in the range of slight depolarizations the potassium currents were not detectably enlarged by tolperisone (see Fig. 3)

On the whole, therefore, our findings have revealed no similarity between the actions of tolperisone and those of the potassium-channel blocking agent 5-MOP, mentioned at the outset as an antispastic agent. The sodium-channel blocking produced by 5-MOP is negligible in comparison to its much stronger blocking of potassium channels (Bohuslavizki et al 1994b), which is not true of tolperisone. 5-MOP also differs from tolperisone in that the latter effect is accompanied by a markedly phasic time course of the potassium currents that are not blocked. Hence

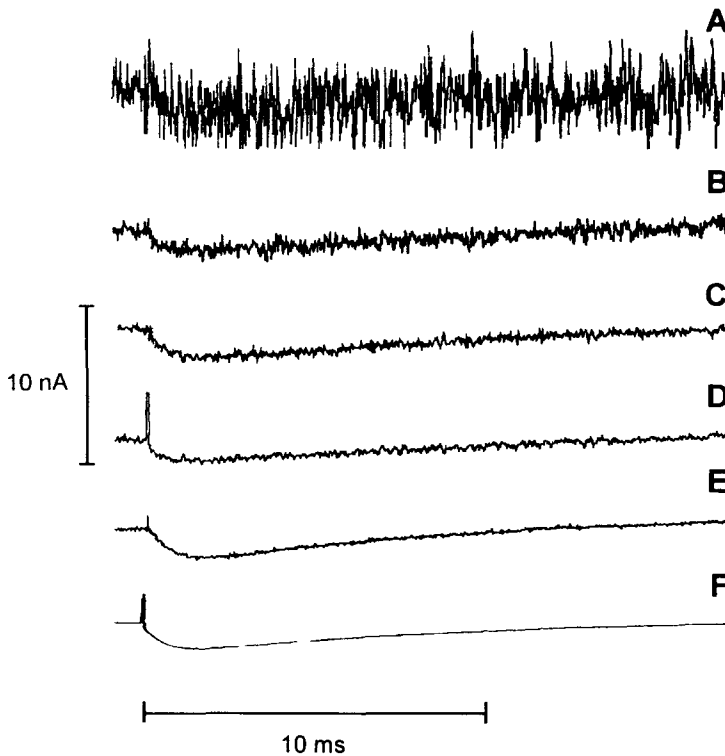


Figure 9. Progressive noise attenuation as demonstrated by recordings elicited at $V = 30$ mV and digitized at 250 kHz (12 bit) **A.** anti-aliasing filter (100 kHz), so-called “raw data” **B.** effect of additional low pass filtering (Bessel, fourth order, corner frequency 20 kHz) **C.** effect of additional digital filtering window width 5 data points **D.** effect of window widening 17 data points **E.** effect of averaging of 16 recordings at 1 Hz as compared to **B.**, i.e. without digital filtering **F.** effect of additional digital filtering (window width 17 data points) as compared to **E.** maximum noise attenuation

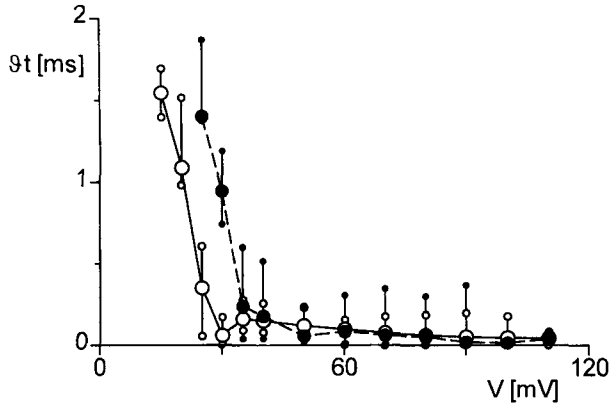


Figure 10. Potential dependence of the delay time δt of the experimental setup. Open symbols: normal Ringer solution, filled symbols: under tolperisone. Linear interpolation. Medians and ranges, $N = 12$.

with respect to the blocking of potassium channels, whereas 5-MOP is an open channel blocker (Düring et al. 2000), tolperisone certainly is not.

Observations on the reliability of our results. Regarding the reliability of ionic current recordings in Ranvier nodes and in particular, their least square fitting by the corresponding equations of the Hodgkin-Huxley formalism, many reports have been published (for references, see Düring et al. 2000); and the problem of distinguishing sodium from potassium currents in the total current recordings has also been satisfactorily solved (Hinck et al. 2001).

However, because of an unfavourable signal/noise ratio it has not yet been possible to carry out curve fitting with current recordings elicited by depolarization weaker than about $V = 40$ mV. It was only by suitably employing all technically possible methods of noise suppression that, in the most favourable case, it was possible to extend the investigated potential range to $V = 15$ to 20 mV. The additional data so obtained, in comparison to previous studies, are nevertheless not of equal reliability. The first reason is that the prerequisites for validity of Eqs. (1) and (4), namely $h_\infty = 0$ and $n_o = 0$, respectively, are met only imprecisely, as shown in Figs. 4D and 5A. Furthermore, the transfer function of the very simply structured digital filters we used, in particular for relatively broad data windows and severe damping (> 15 dB), has such an unsatisfactory shape that this kind of filtering was used only rarely. That we are likely to have been sufficiently cautious is evident in Fig. 9, from comparison of the recordings *C* and *D* (5 and 17 data points, respectively) with recording *B*.

Discussions of the so-called delay time δt of the measurement system have been published previously (Düring et al. 2000; Hinck et al. 2001). Fig. 10 (open symbols) shows the marked potential-dependence of δt , which once again emphasizes how

problematic it still is, however perfected the technology, to draw any conclusions about rapid components in current recordings, especially in the region of negative membrane resistances at the Ranvier node. Whether the observed rightward shift of the steep rise of δt under weak depolarization is a tolperisone-specific effect – that is, whether δt is not merely a purely technical parameter of the measurement system – has not been tested.

There is a conspicuously large scatter in our data on current kinetics. In this regard we found no difference between the rapid sodium-current kinetics in comparison to the slower potassium-current kinetics (see Fig. 4A,B and Fig. 5B,C). Therefore one potential explanation, an insufficient temporal resolution in the measurement system, can probably be eliminated; the same also applies to the use of gallamine to separate the sodium and potassium currents (see Hinck et al. 2001). As mentioned above, there is a difference between the kinetics of ion currents in motor and in sensory axons (Bretag and Stampfli 1975; Stämpfli and Hille 1976). Because in the present experiments, contrary to customary practice, we made a point of not distinguishing between motor and sensory axons, we consider it possible that the broad scatter reflects the dissimilarity of the axons involved.

References

- Albers M, Bohuslavizki K H, Koppenhofer E (1989) High standard one-loop potential clamp device for Ranvier nodes *Gen Physiol Biophys* **8**, 409–433
- Århem P, Frankenhaeuser B (1974) Local anesthetics effects on permeability properties of nodal membrane in myelinated nerve fibres from *Xenopus* Potential clamp experiments *Acta physiol scand* **91**, 11–21
- Bautz'as Ch, Bohuslavizki'is K H, Ditzen'as G, Gerst'as F, Hansel'is W, Hinck-Kneip'as Chr, Koppenhofer'is E, Ramanauskas J, Reimers'as A (1995) Ruta – naujos galumybes išsėtinei sklerozei gydymui *Medicina (Kaunas)* **31**, 52–55
- Bautz Ch, Bohuslavizki K H, Ditzen G, Gerst F, Hansel W, Hinck-Kneip Ch, Koppenhofer E, Reimers A (1996) Ruta – Un nuevo método en la terapia sintomática de la esclerosis múltiple *Rev Chil Neuro-Psiquiat* **34**, 57–60
- Bethge E W, Bohuslavizki K H, Hansel W, Kneip A, Koppenhofer E (1991) Effects of some potassium channel blockers on the ionic currents in myelinated nerve *Gen Physiol Biophys* **10**, 225–244
- Bohuslavizki K H, Hansel W, Kneip A, Koppenhofer E, Reimers A, Sanmann K (1993a) Blocking of potassium channels in Ranvier nodes by 4, 5, 6, 7-substituted benzofurans and its significance on demyelinating diseases *Gen Physiol Biophys* **12**, 293–301
- Bohuslavizki K H, Hinck-Kneip Ch, Kneip A, Koppenhofer E, Reimers A (1993b) Reduction of MS-related scotomata by a new class of potassium channel blockers from *Ruta graveolens* *Neuro-Ophthalmol* **13**, 191–198
- Bohuslavizki K H, Kneip A, Koppenhofer E (1994a) State-of-the-art potential clamp device for myelinated nerve fibres using a new versatile input probe *Gen Physiol Biophys* **13**, 357–376
- Bohuslavizki K H, Hansel W, Kneip A, Koppenhofer E, Niemoller E, Sanmann K (1994b) Mode of action of psoralens, benzofurans, acridinons, and coumarins on the ionic currents in intact myelinated nerve fibres and its significance in demyelinating diseases *Gen Physiol Biophys* **13**, 309–328

- Bohuslavizki K H, Ditzen G, Gerst F, Hansel W, Koppenhofer E, Reimers A, Sanmann K (1995) Psoralens – a new class of potassium channel blockers for the symptomatic treatment of multiple sclerosis *Pflugers Arch* **430**, R 36
- Bretag A H, Stampfli R (1975) Differences in action potentials and accommodation of sensory and motor myelinated nerve fibres as computed on the basis of voltage clamp data *Pflugers Arch* **354**, 257–271
- Courtney K R (1975) Mechanism of frequency-dependent inhibition of sodium currents in frog myelinated nerve by lidocaine derivative GEA 968 *J Pharmacol Exp Ther* **195**, 225–236
- Ditzen G, Gerst F, Hansel W, Koppenhofer E (1995) Kaliumkanal-Blocker – ein neuer Ansatz zur symptomatischen Therapie der multiplen Sklerose *Dtsch Med Wochenschr* **120**, 1061–1062
- Dodge F A, Frankenhaeuser (1958) Membrane currents in isolated frog nerve fibre under voltage clamp conditions *J Physiol (London)* **143**, 76–90
- During T, Hansel W, Koppenhofer E, Wulff H (1997) Psoralens – the new class of K⁺-channel blockers for the specific, symptomatic treatment of demyelinating diseases *Pflugers Arch* **434**, R 112
- During T, Gerst F, Hansel W, Wulff H, Koppenhofer E (2000) Effects of three alkoxy-psoralens on voltage gated ion channels in Ranvier nodes *Gen Physiol Biophys* **19**, 345–364
- Farkas S, Tarnawa I, Berzsenyi P (1989) Effects of some centrally acting muscle relaxants on spinal root potentials a comparative study *Neuropharmacology* **21**, 161–173
- Fels G (1996) Tolperisone evaluation of the lidocaine-like activity by molecular modeling *Arch Pharm Pharm Med Chem* **329**, 171–178
- Frankenhaeuser B (1959) Steady state inactivation of sodium permeability in myelinated nerve fibres of *Xenopus laevis* *J Physiol (London)* **148**, 671–676
- Frankenhaeuser B (1960) Quantitative description of sodium currents in myelinated nerve fibres of *Xenopus laevis* *J Physiol (London)* **151**, 491–501
- Frankenhaeuser B (1962) Potassium permeability in myelinated nerve fibres of *Xenopus laevis* *J Physiol (London)* **160**, 54–61
- Frankenhaeuser B (1963) A quantitative description of potassium currents in myelinated nerve fibres of *Xenopus laevis* *J Physiol (London)* **169**, 424–430
- Hansel W, Koppenhofer E, Wulff H (1998) Psoralene – eine neue Klasse von Kaliumkanalblockern zur spezifischen symptomatischen Therapie von Markscheiden-erkrankungen *Schweiz Arch Neurol Psychiatr* **149**, 81
- Hift St, Sluga-Gasser E (1962) Contribution to the problem of conservative therapy in cases of spastic paralysis *Wiener Med Woch* **112**, 358–362
- Hinck D, Koppenhofer E (1997) Effects of tolperisone on the excitation process in myelinated axons *Pflugers Arch* **433**, R139
- Hinck D, Wulff H, Koppenhofer E (2001) Gallamine triethiodide selectively blocks voltage-gated potassium channels in Ranvier nodes *Gen Physiol Biophys*, **20**, 83–95
- Honerjager P (1968) Die repetitive Aktivität motorischer und sensibler markhaltiger Nervenfasern des Frosches *Pflugers Arch* **303**, 55–70
- Jellinger K (1984) Zur Behandlung der Spastizität bei multipler Sklerose – Ergebnisse einer Doppelblindstudie mit Tizanidin und Diazepam In *Die klinische Wertung der Spastizität* (Eds B Conrad, R Benecke, J Bauer), pp 171–184, Schattauer, Stuttgart
- Koppenhofer E (1967) Die Wirkung von Tetraäthylammoniumchlorid auf die Membranstrome Ranvierscher Schnurringe von *Xenopus laevis* *Pflugers Arch* **293**, 34–55

- Koppenhofer E, Ditzen G, Gerst F, Reimers A (1995) Kaliumkanalblocker in der Neurologie 5-MOP zur Behandlung MS-bedingter Funktionsdefizite TW Neurol Psychiatr **9**, 585—591
- Lehoczy T (1961) A new muscle relaxant (mydocalm) in neurological affections Ther Hung **9**, 10—12
- Matthews P B C, Rushworth G (1957) The relative sensitivity of muscle nerve fibres to procaine J Physiol (London) **135**, 263—269
- Mix E, Wissel K, Wulff H, Rolfs A, Hansel W, Düring T, Koppenhofer E (1998) K⁺ channel block by psoralens: a role for immunosuppression in experimental autoimmune encephalomyelitis (EAE)? Mult Scler **4**, 307
- Morikawa K, Oshita M, Yamazaki M, Ohara N, Mizutani F, Kato H, Ito Y, Kontani H, Koshiura R (1987) Pharmacological studies of the new centrally acting muscle relaxant 4-ethyl-2-methyl-3-pyrrolidinopropiophenone hydrochloride Arzneimittel-Forsch /Drug Res **37** (I), 331—336
- Ono H, Fukuda H, Kudo Y (1984) Mechanisms of depressant action of muscle relaxants on spinal reflexes: participation of membrane stabilizing action J Pharm Dyn **7**, 171—176
- Raymond S A (1992) Sub-blocking concentrations of local anesthetics: effects of impulse generation and conduction in single myelinated sciatic nerve axons in frog Anesth Analg (N Y) **75**, 906—921
- Sachs L (1984) Applied statistics: A handbook of techniques Springer, New York
- Sotgiu M L, Lacerenza M, Marchettini P (1992) Effect of systemic lidocaine on dorsal horn neuron hyperactivity following chronic peripheral nerve injury in rats Somatosens Motor Res **9**, 227—233
- Stampfli R, Hille B (1976) Electrophysiology of the peripheral myelinated nerve In Frog Neurobiology (Eds R Llinas, N Precht), pp 3—32, Springer, Berlin
- Strichartz G R (1987) Local anesthetics In Handbook of experimental Pharmacology (Eds G V Born, A Farah, H Herken, A D Welch), Vol 81, Springer, Berlin
- Szobor A (1993) Mydocalm's thirty-year clinical use Ther Hung **41**, 3—12
- Waxman S G (1987) Conduction properties and pathophysiology of myelinated and non-myelinated nerve fibres In Handbook of clinical neurology (Eds P J Vinken, G W Bruyn), Vol 7 (51) Neuropathies, (Ed W B Matthews), pp 41—62, Elsevier, Amsterdam
- Wissel K, Wulff H, Düring T, Rolfs A, Hansel W, Koppenhofer E, Mix E (1998) K⁺ channel blocking psoralens inhibit the immune response of lymph node cells (LNC) of Lewis rats with experimental autoimmune encephalomyelitis (EAE) Eur J Neurosci **10** (Suppl 10), 164
- Wulff H, Koppenhofer E, Hansel W (1998a) Potassium channel blocking psoralens, benzofurans, acridones and coumarins for the treatment of multiple sclerosis and related diseases Current Research in Ion Channel Modulators **3**, 207—212
- Wulff H, Rauer H, Düring T, Hanselmann Ch, Ruff K, Wrisch A, Grissmer S, Hansel W (1998b) Alkoxypsoralens, novel nonpeptide blockers of Shaker-type K⁺ channels: synthesis and photoreactivity J Med Chem **41**, 4542—4549
- Young R R (1994) Spasticity: a review Neurology **44**, (Suppl 9), 12—20
- Zaciu C, Koppenhofer E, Maskalunas R (1996) Reliability of ionic current measurements in Ranvier nodes Gen Physiol Biophys **15**, 89—107